Functionalized polytriazoles on graphene oxide-supported copper (I) complex as an effective reusable catalyst for sonochemical click synthesis of triazoles in aqueous media

Hossein Naeimi, Zahra Ansarian

PII: S0020-1693(17)30758-2
DOI: http://dx.doi.org/10.1016/j.ica.2017.06.057
Reference: ICA 17706

To appear in: *Inorganica Chimica Acta*

Received Date: 13 May 2017
Accepted Date: 26 June 2017

Please cite this article as: H. Naeimi, Z. Ansarian, Functionalized polytriazoles on graphene oxide-supported copper (I) complex as an effective reusable catalyst for sonochemical click synthesis of triazoles in aqueous media, *Inorganica Chimica Acta* (2017), doi: http://dx.doi.org/10.1016/j.ica.2017.06.057

Functionalized polytriazoles on graphene oxide-supported copper (I) complex as an effective reusable catalyst for sonochemical click synthesis of triazoles in aqueous media

Hossein Naeimi*, Zahra Ansarian

Department of Organic Chemistry, Faculty of Chemistry, University of Kashan, Kashan, 87317-51167, I.R. Iran; Fax: +98-03155912397; Tel: +98-03155912388;

E-mail: naeimi@kashanu.ac.ir

Abstract

In the present study, a copper complex immobilized on graphene oxide was synthesized as a novel, green, highly efficient and reusable heterogeneous catalyst. Then, the synthesis of *β*-hydroxy-1,2,3-triazole derivatives were performed by the employment of GO@polytriazole-Cu as catalyst under ultrasound irradiation to afford the desired products in high yields and short reaction times. Also, in this protocol the catalyst could be easily recovered and reused several times without any significant loss of its catalytic activity.

Keywords: Ultrasound, Graphene oxide, Triazole, Catalyst, Click reaction, Complex.

1. Introduction

One of the key benefits of green chemistry is the replacement of the conventional heating techniques with environmentally safe process such as the use of ultrasound. It has been used to increase the reaction rates and give higher yields in a lot of organic reactions [1]. On the other hand, catalysis is one of the substantial bases of green chemistry [2]. Elimination of trace amounts of catalyst from the end product is necessary since metal contamination is highly regulated, especially by the pharmaceutical industry. To overcome these problems, scientists have investigated a numerous range of strategies and the use of heterogeneous catalyst systems appears to be the best logical solution [3]. Recycling of organocatalysts is a significant aspect in green chemistry. Thus, recent attainments in chemical performance have focused on use of heterogeneous catalysts in organic reactions.

1,2,3-Triazole derivatives are usually acquired via the Huisgen's azide–alkyne cycloaddition (CuAAC reaction). Several copper sources have been demonstrated for the CuAAC, containing simple halide salts and coordination complexes in homogeneous or heterogeneous form [4-7].

One-pot synthesis of 1,2,3-triazoles has been reported through heterogeneous catalytic systems such as aminopropyl-silica-supported Cu nanoparticles [8], chitosan stabilized copper iron oxide nanocomposite [9], $CuFe_2O_4$ nanoparticles [10], carbon-supported copper nanomaterials [11], Cu[N^2,N^6-bis(2-hydroxyphenyl) pyridine-2,6-dicarboxamidate] [12].

A more generally suitable strategy that prevents the contamination of the metals in the reaction products is the immobilization of the catalyst to a support such as mesoporous silica [13, 14], zeolites [15, 16], polymers [17, 18], and activated carbons [19], which can be easily removed from the final product, and ideally be reused for subsequent reactions. Among these support systems, graphene oxide is a special support used in the preparation of heterogeneous catalysts

[20, 21]. Graphene, a two dimensional (2D) structure of sp^2-bonded carbon atoms, has been widely used in organic synthesis, materials chemistry, and biomedicine because of its high specific surface area, chemical and thermal stability, very high electrical conductivity, non-toxicity, flexibility.[22, 23] Graphene oxide surface contains polar functional groups including alcohols, epoxides, and carboxylic acids [23-26]. Moreover, these functional groups have been shown to be reactive toward some reactive groups such as isocyanate [27], chlorosulfonic acid as the sulfonating reagent [28] and amine groups [29]. Functionalization of graphene oxide is the important route to gain well interfacial bonding between graphene oxide sheets and functional active site.

The various ligands have been employed in the preparation of copper complex as catalysts in CuAAC reactions including (substituted) bipyridines [30, 31], (substituted) 1,10-phenanthroline[30], tris(2-dioctadecylaminoethyl) amine[32], tris(1-benzyl-1H-1,2,3-triazol-4-yl)-methanol[33]. Due to the interesting properties of GO as a support for the preparation of heterogeneous catalytic system, herein, we report a preparation of GO-supported copper catalyst, include 1,2,3-triazoles as copper (I)-stabilizing ligands in catalysis to prepare the β-hydroxy-1,2,3-triazoles under ultrasound irradiation in water at room temperature.

2. Results and discussion

2.1. Preparation and characterization of the catalyst

The structures of heterogeneous Cu(I) complex and the intermediate steps were characterized by Fourier transform infrared spectroscopy (FT-IR), Energy-dispersive X-ray spectroscopy (EDX), X-ray diffraction(XRD), Field emission scanning electron microscopy (FE-SEM), Atomic-force microscopy(AFM) andInductively coupled plasma (ICP) analyses.

Due to the fascinating properties of GO as support for the preparation of heterogeneous catalytic system, we describe a preparation of GO-supported copper catalyst, include 1,2,3-triazoles as copper(I)-stabilizing ligands (Scheme 1).

.

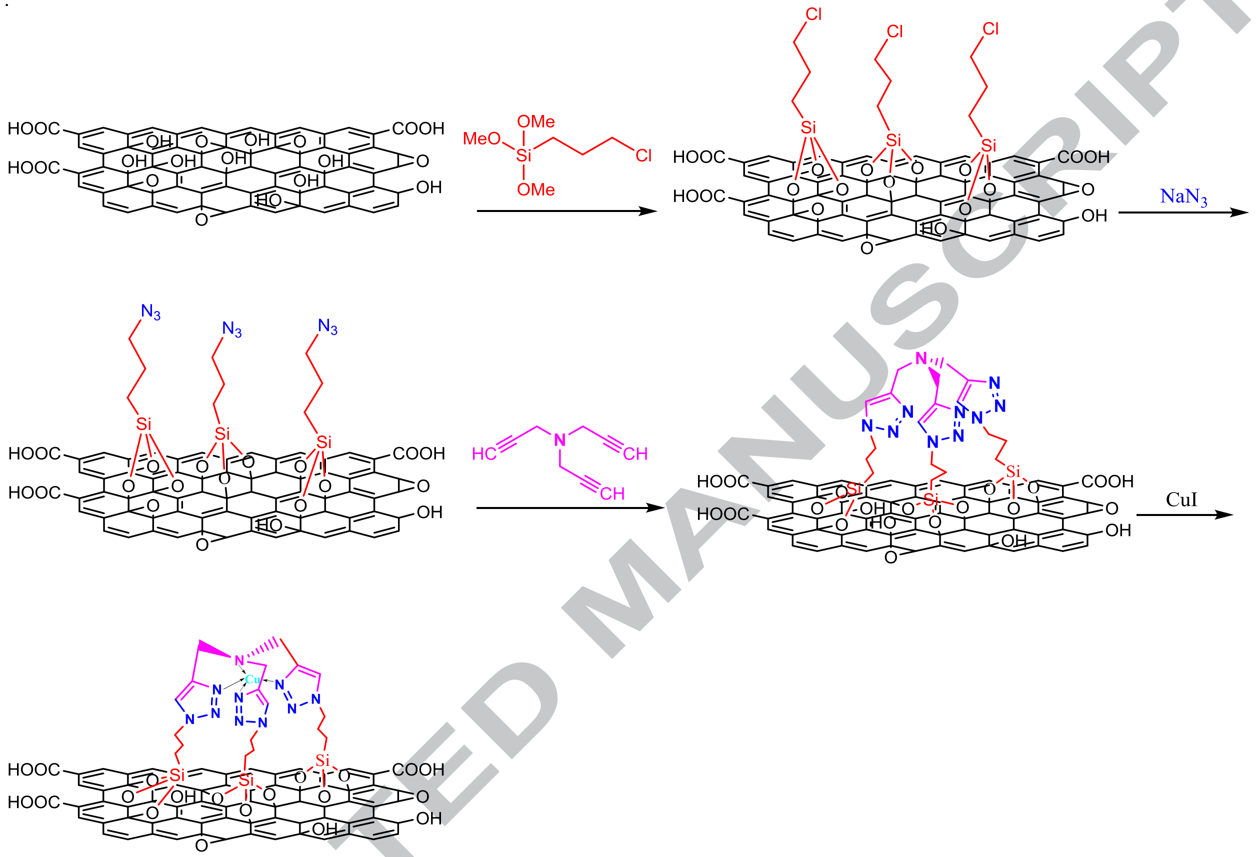

Scheme1. Preparation of GO@PTA-Cu organocatalyst

Figures **1a–e** indicates the FT-IR spectra of graphite, GO, GO@CTS, GO@N_3 and 1,2,3-triazole-functionalized GO (GO@PTA), respectively. The FT-IR spectrum of natural graphite powder has been exhibited in Fig. 1a. Figure1b shows the FT-IR spectrum of GO powder. The stretching vibration at 3398 cm^{-1} in the GO (Fig. 1b) refers to the OH groups, and the absorption band at 1717 cm^{-1} corresponds to C=O groups. As indicated in Fig. 1b, the absorption peaks at 1640 cm^{-1} and 1056 cm^{-1} are assigned to carbon–carbon double bonds and C-O, respectively. The presence of numerous hydroxyl groups on the GO, provide active sites for the bonding between GO sheets and silane. Figure **1c** shows the FT-IR spectrum of the CPTES coated graphene oxide. As can be seen in this Figure, the FT-IR absorption peak at 1045 cm^{-1} representing the Si–O–C bond and the vibrational bands at 2926 cm^{-1} and 2854 cm^{-1} are attributed to CH_2 groups. Also, the presence of peak at 695 cm^{-1} is represented the C-Cl bond, which indicated the successful coating of CPTES onto the graphene oxide through chemical bonding. The Fig. **1d** is shown the absorption peak of azide groups at 2098 cm^{-1}. Figure **1e** shows the FT-IR spectrum of the 1,2,3-triazole-functionalized GO. In this Figure, the disappearance of peak at 2098 cm^{-1} indicated the successful azide-alkyne coupling reaction on the nanosheets. Moreover, the N=N stretching absorption for triazole compounds appeared nearly around 1457 cm^{-1}.

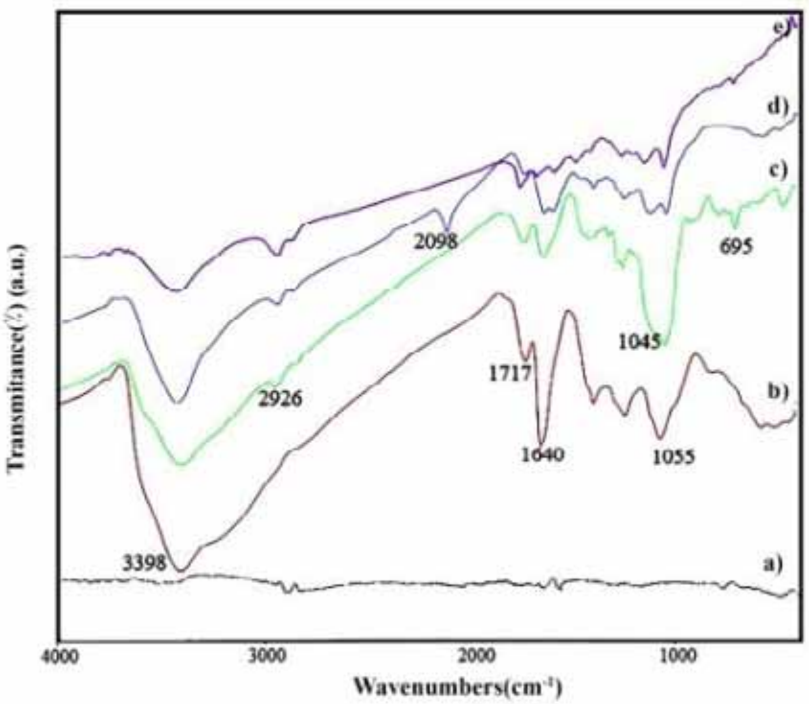

Fig. 1. FT-IR spectra of (a) graphite, (b) GO, (c) GO@CTS, (d) GO@N_3 and (e) GO@PTA

XRD patterns were analyzed to realize the phase structure of GO. Figure **2a-c** shows XRD patterns of graphite, GO and GO@PTA-Cu, respectively. The graphite powder shows a sharp peak at 2Θ= 26° (Figure **2a**), corresponding to the interlayer spacing (d-spacing= 0.335 nm). The exfoliated graphene oxide shows a broad peak at about 2Θ = 26.5° and a peak at 2Θ = 12° (d-spacing=0.78 nm) (Figure **2b**). The enhancement in d spacing is due to the intercalation of water molecules and the formation of oxygen-containing functional groups between the layers of the graphite. After the surface covalent functionalization of GO with CPTMS, click coupling process and finally production of the GO@PTA-Cu catalyst, the diffraction peak at 2Θ=12◦ compared to GO was disappeared that indicated the increasing of interlayer distances (Figure 2c).

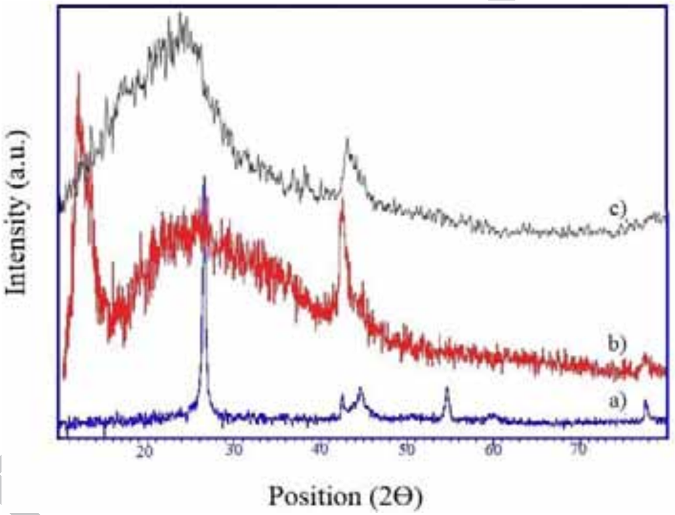

Fig. 2. XRD patterns of (a) graphite, (b) GO and (c) GO@PTA-Cu

The FE-SEM images of GO, GO@PTA-Cu are shown in Figure 3. Different morphologies were observed for GO nanosheets and prepared catalyst. This images confirmed that two dimensional GO nanosheets can be produced via exfoliation of suspended graphite oxide.

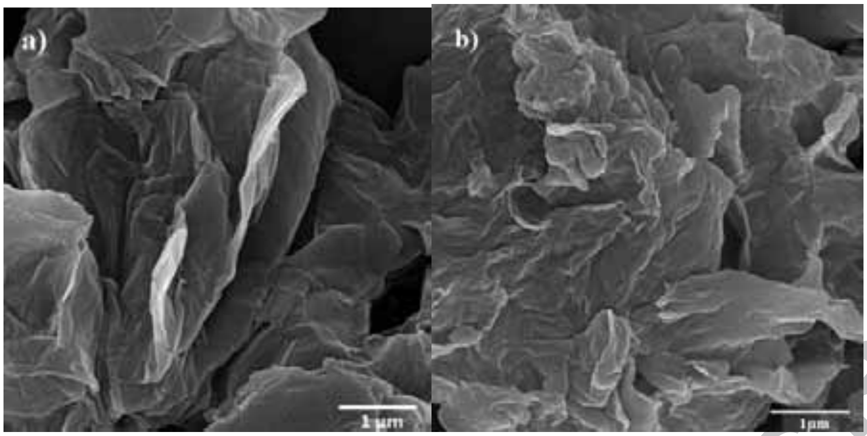

Fig. 3. FE-SEM images of (a) GO and (b) GO@PTA-Cu

Atomic force microscopy (AFM) is employed to observe the morphology of GO nanosheets and measure their thickness. The AFM images of the GO and GO@PTA-Cu easily confirm the wrinkled 2D characteristic of the GO nanosheets. The images indicate that the thicknesses of GO was approximately 0.9 to 1.5 nm, corresponding to structures with 1 to 2 layers (Figure **4a**). After the surface functionalization, the thickness of sheets is increased to 4.3 nm (Figure **4b**). The addition in thickness of functionalized GO nanosheets is perhaps caused by the organic compounds grafted on the graphene oxide sheets, indicating the successful functionalization of GO.

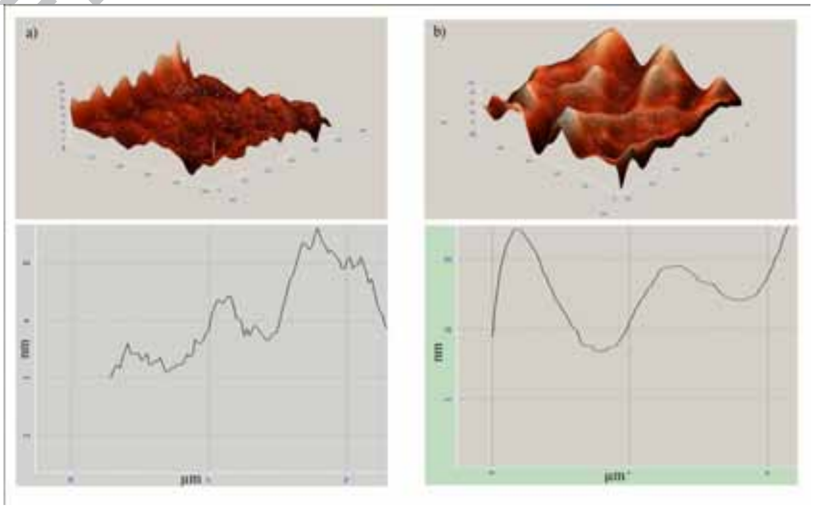

Fig. 4. AFM images of (a) GO nanosheets and (b) GO@PTA-Cu

The Cu content of GO@PTA-Cu catalyst was determined by an inductively coupled plasma (ICP) analyzer. According to the obtained results from ICP analysis, it was revealed the presence of 1.1% copper on the catalyst. Also, to support the mentioned observation, the catalyst was subjected to energy dispersive X-ray. The EDX analysis of GO and GO@PTA-Cu catalyst confirmed the presence of organosilane and copper on their regions (Figure **5a,b**).

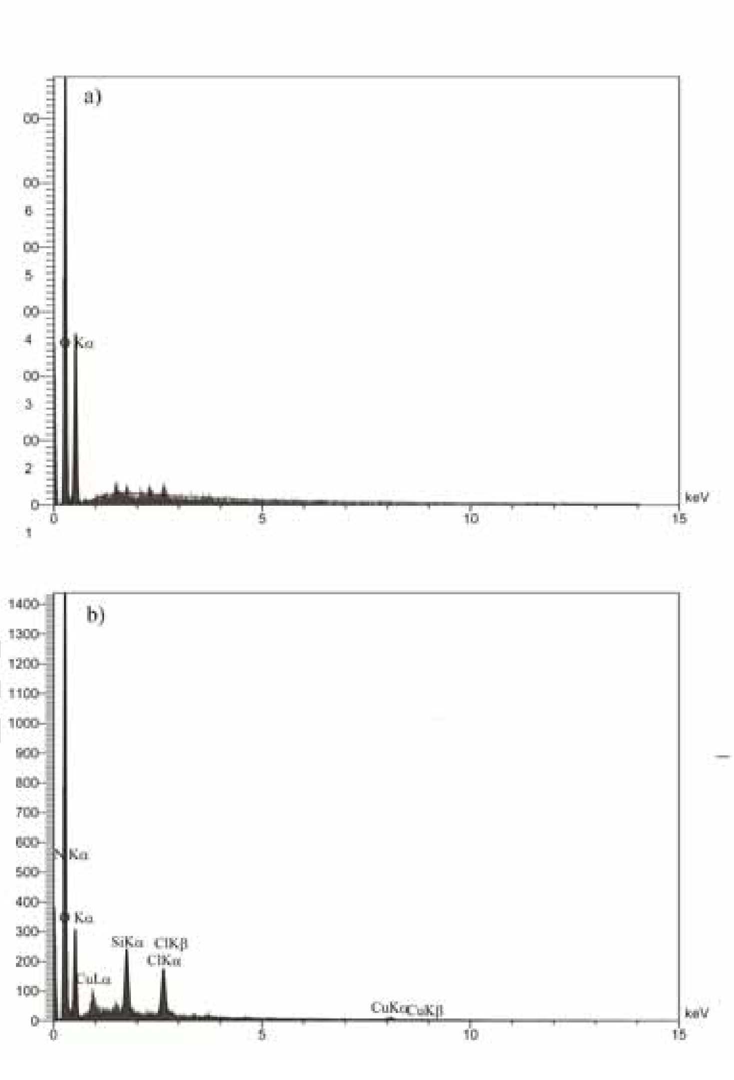

Fig. 5. EDS patterns of (a) GO and (b) GO@PTA-Cu

TGA was further employed to confirm the successful anchoring of organic groups on the surface of GO. As shown in Figure 6, Below 260 °C, there was a mass loss (42%) that was attributable to the removal of adsorbed water firstly and oxygen-containing functional groups on the GO surface. Around 260–610 °C, a reduction occurred (24%), which is attributed to the covalency of organic groups.

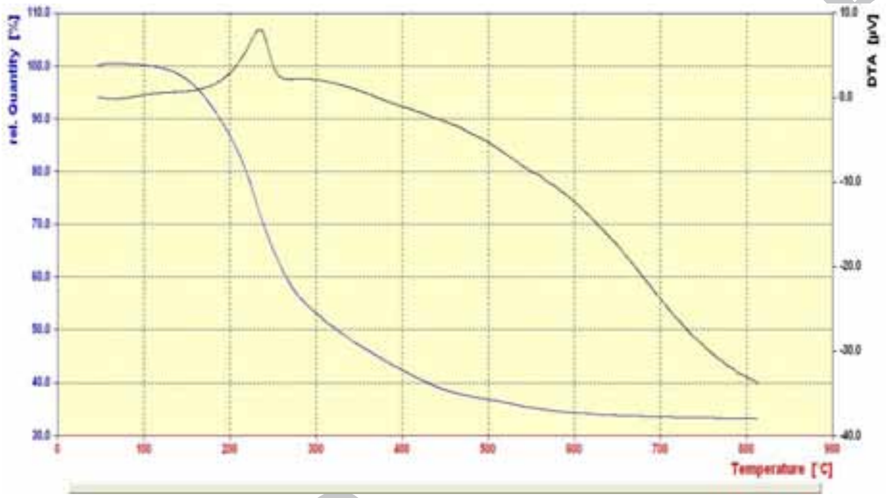

Fig. 6. TGA curve of GO@PTA-Cu

Thermogravimetric analysis can evaluate the amount of functional groups per carbon atoms.[34] To estimate the amount of functionalization, weight loss values were used together with the molecular weight of the different groups and equation (1) was applied.

$$X = \frac{\mathrm{R}(\%).\mathrm{Mw}\ (\mathrm{g/mol})}{\mathrm{L}\ (\%).12\ (\mathrm{g/mol})} \qquad (1)$$

where X stands for the number of carbon atoms in GO@PTA per covalent functional group, R (%) is the residual mass at 610 °C in the TGA plot, L (%) is the weight loss between 260–610 °C, and Mw is the molecular weight of the organic groups on the surface of GO.

According to equation 1, organic groups on the surface of GO measurements indicated that there is one functional group every approximately 70 carbon atoms.

2.2. *Investigation of catalyst activity*

Initially, the reaction parameters such as catalyst amount (%), solvent and sonication time (min) were optimized in the reaction of styrene oxide (1 mmol), phenylacetylene (1 mmol), NaN_3 (1.1 mmol) as the model reaction (Scheme 2).

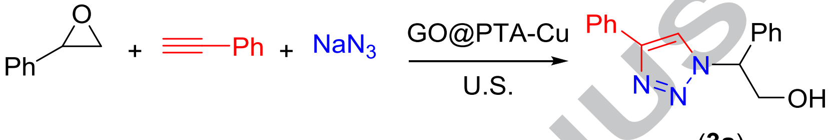

(**3a**)

Scheme 2. Synthesis of 2-phenyl-2-(4-phenyl-1H-1,2,3-triazol-1-yl)ethanol (**3a**).

To choose the medium of the reaction, different solvents were screened in the model reaction. It was found that the reaction with using H_2O after 7 min resulted in higher yield (Table 1). Moreover, the reactions were clean in water compared to those in organic solvents. The results are shown in Table 1.

Table 1. Solvent optimization for the synthesis of **3a** in the model reaction[a]

Entry	Solvent	Time (min)	Yield[b] (%)
1	H_2O	7	95
2	EtOH	7	70
3	H_2O: MeOH (50:50)	9	85
4	$PhCH_3$	13	35

5	CH_2Cl_2	13	27
6	*n*-Hexane	12	15

[a] Reaction conditions: styrene oxide (1 mmol), phenylacetylene (1 mmol), NaN_3 (1.1 mmol), GO@PTA-Cu (10mg, 0.017 mol%), under ultrasound conditions, [b] Isolated yields.

The amount of GO@PTA-Cu as a catalyst for this reaction was also evaluated. (Table 2) The model reaction was carried out in the presence of different mole amounts of catalyst. The best result was observed with 10 mg (Cu, 0.0017mmol) of the catalyst and the catalyst afforded 95% yield of the product **3a** at 7 min in water under ultrasound irradiation. No product was observed in the absence of the catalyst Table 2, entry 1).

Table 2. The optimization of GO@PTA-Cu catalyst amount in the model reaction[a]

Entry	Catalyst (mg)	Cu(mmol)	Time (min)	Yield[b] (%)
1	0	-	30	-
2	2	0.00034	10	73
3	5	0.00086	7	92
4	10	0.0017	7	95
5	20	0.0034	8	90

[a]Reaction conditions: styrene oxide (1 mmol), phenylacetylene (1 mmol), NaN_3 (1.1 mmol), H_2O, GO@PTA-Cu (0.017%), under ultrasound conditions, [b] Isolated yields.

The effect of ultrasonic irradiation frequency on this reaction was also investigated. In this regard, the sample model reaction was carried out at different irradiation powers in the range of 20–55 W and without ultrasound (Table 3).

As can be seen, without exposing the reaction to ultrasound irradiation, the product was not obtained at room temperature for 120 min. (Table 3, entry 1). Moreover, the effect of ultrasonic irradiation of different powers was examined. It was observed that reaction in the presence of GO@PTA-Cu and ultrasonic irradiation at power of 45 W acquired the best yield of product, with 95 % isolated yield after 7 min (Table 3, entry 4). It means that the ultrasound can be accelerated the rate of reaction and formation of pure products in high yields. The effects of ultrasound on chemical reactions is related to the formation, growth and collapse of the hole in a liquid leading to localized hot spots with high temperature, high pressure. Therefore, ultrasonic irradiation can be employed as an alternative energy source for organic reactions ordinarily accomplished by heating.

Table 3. The influence of ultrasonic irradiation on the synthesis of **3a** in the model reaction[a]

Entry	Power	Time (min)	Yield[b] (%)
1	Silent	120	-
2	20	20	55
3	30	13	70
4	45	7	95
5	55	7	95

[a] Reaction conditions: styrene oxide (1 mmol), phenylacetylene (1 mmol), NaN_3 (1.1 mmol), GO@PTA-Cu (10mg, 0.017 mol%), under various ultrasound irradiation power at room temperature,[b] Isolated yields.

After optimization of the reaction conditions, we performed these conditions for a series of different aryl and alkyl-substituted oxiranes (**1a-j**) and terminal alkynes (**2a,b**) to probe the versatility of the protocols under GO@PTA-Cu catalysis. The results are summarized in Table 4. We first investigated the reaction of aryl-substituted epoxides with phenylacetylene (Table 4, entries 1,2). The aryl-substituted epoxides **1a** and **1b** reacted rapidly, affording triazoles **3a** and **3b**, respectively, in high yields and short reaction times and with reverse regioselectivity to that displayed by the alkyl-substituted epoxides. Subsequently, we examined the reaction between aliphatic epoxides and phenylacetylene (Table 4, entries 3-10). In these cases, it was observed a decrease in yield and increase in reaction time than the aryl-substituted epoxides. The formation of bis-triazoles **3h** from **1h** and **1i** in this reactions can be due to the existence of good leaving groups (OTs, Cl) in the primary epoxides (Table 4, entries 8,9). The consumption of the internal alkynes in this procedure led to the formation of product which resulted from the ring opening of epoxide, without forming any triazole product (Table 4, entry 12). Furthermore, the structures of these products were confirmed by ^{1}H NMR and ^{13}C NMR spectra.

Table 4. Synthesis of β-hydroxy-triazoles catalyzed by GO@PTA-Cu

Entry	Alkyne (R_2)	Epoxide	Product	T (min)	Yield^b(%)	TON^c	TOF^d (h^{-1})
1	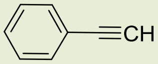	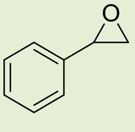 (**1a**)	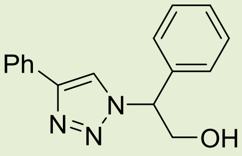 (**3a**)	7	95	549	4692
2	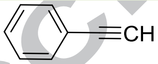	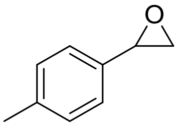 (**1b**)	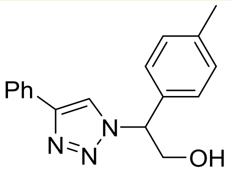 (**3b**)	7	95	549	4692
3	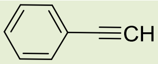	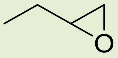	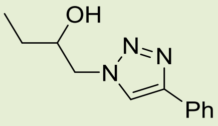	13	92	531	2447

		(1c)	**(3c)**				
4	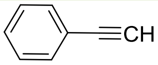	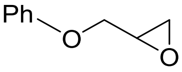 **(1d)**	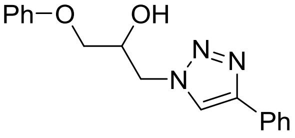 **(3d)**	14	93	537	2304
5	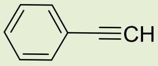	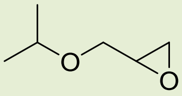 **(1e)**	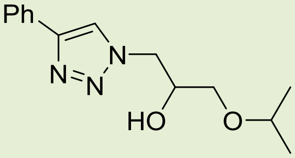 **(3e)**	17	92	531	1876
6	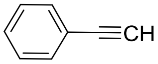	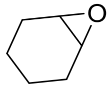 **(1f)**	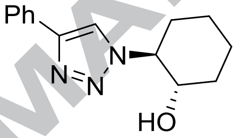 **(3f)**	12	90	520	2600
7	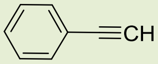	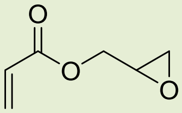 **(1g)**	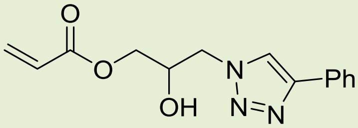 **(3g)**	20	85	491	1474
8[e]	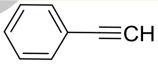	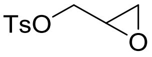 **(1h)**	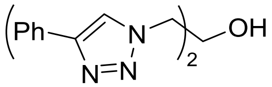 **(3h)**	10	90	520	3113

9 ^{e}	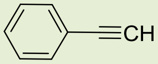	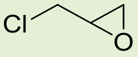 (**1i**)	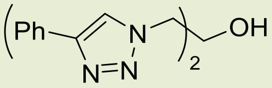 (**3h**)	17	82	473	1671
10	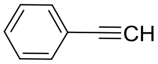	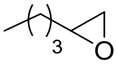 (**1j**)	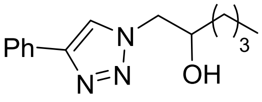 (**3i**)	16	90	520	1947
11	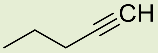	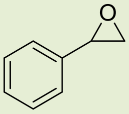 (**1a**)	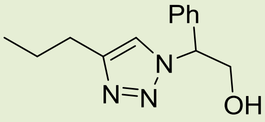 (**3j**)	10	90	520	3114
12	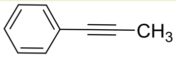	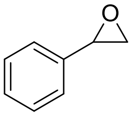	–	30	-	-	-

[a] General reaction conditions: 1 (1 mmol), 2 (1 mmol), NaN_3 (1.1 mmol), GO@PTA-Cu (0.017 mol%, 10mg), H_2O, under ultrasound conditions,[b] Isolated yields. [c]TON: mole of formed *β*-hydroxy-1,2,3-triazole per mole of catalyst. [d] TOF (h^{-1}): (mmol of product/mmol of active site of catalyst)/ time of the reaction (**h**). [e] The reaction was done with 1 : 2 : 2 mol ratio of epoxide, alkyne and NaN_3, respectively.

The recovery and reusability of catalysts are highly preferable for the green process. The possibility of recycling the catalyst was investigated through the model reaction under optimized conditions. Upon completion of the reaction, the catalyst was separated by filtration, washed with methanol and drying at 80°C in an oven for 8h. The recycled catalyst could be reused five times with no loss of catalytic activity so that the yields were ranged from 95 to 87 % (Figure 7).

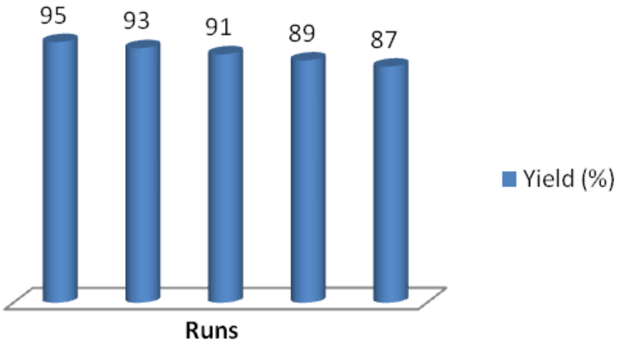

Fig. 7. The reusability of the catalyst GO@PTA-Cu in the synthesis of (3a)

2.3. The proposed mechanism

The suggested mechanism for the formation of β-hydroxy-1,2,3-triazoles includes two routes [35], in which GO@PTA-Cu has a two-fold catalytic impress as a bifunctional catalyst, which incorporates one-pot ring opening and 1,3-dipolar cycloaddition. Firstly, GO@PTA-Cu catalyze the formation of organoazide (II) from epoxide and sodium azide (Scheme 3).

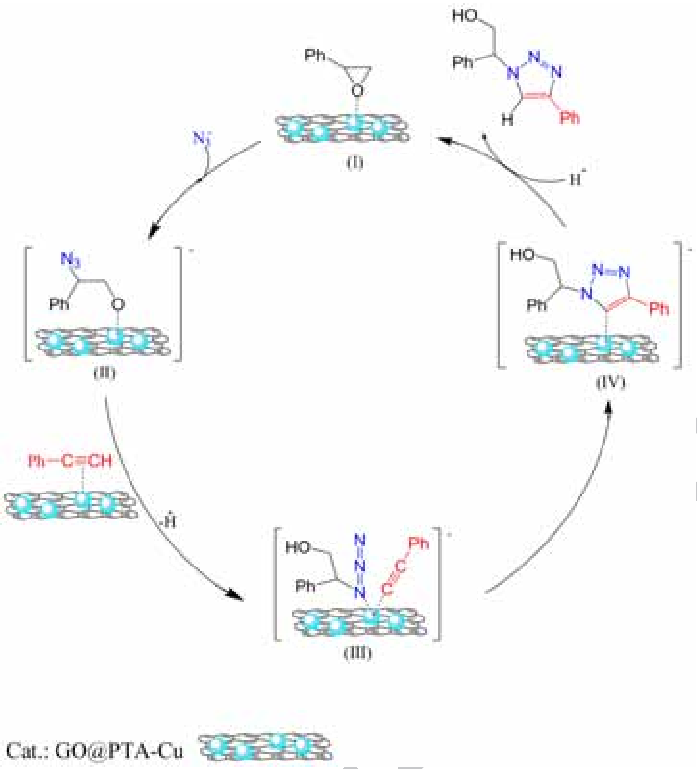

Scheme 3. Proposed mechanism for synthesis of *β*-hydroxy-1,2,3-triazoles

Also, a π-complex is formed between phenylacetylene and GO@PTA-Cu to obtain the copper (I) acetylide intermediate (III) the generation and disappearance of the organoazide intermediate being monitored by TLC. Coordination of the organoazide to the copper center of the acetylide enhances the nucleophilicity of the triple bond and initiates a sequence of steps which finally results in the formation of the new C-N bond between the nucleophilic β-carbon atom of the acetylide and the terminal, electrophilic nitrogen atom of the azide.[36]

Ultimately, after protonation of intermediate (IV), β-hydroxy-1,2,3-triazole is obtained in high yield and short reaction time.

3. Conclusion

In conclusion, we have successfully demonstrated that a straightforward, clean, eco-friendly, efficient and cost-effective synthesis of 1,2,3-triazoles in an aqueous medium water under ultrasound irradiation. Furthermore, in this research we have designed a heterogeneous catalyst based on GO@polytriazole-Cu. These polytriazole ligands on the surface of GO not only stabilize Cu(I) intermediates but also advance the catalytic process. The prepared catalyst was characterized using various techniques such as; FT-IR, FE-SEM, ICP, EDS, AFM and XRD techniques. These results confirmed that the functionalization of GO was performed.

4. Experimental section

4.1 Materials and Apparatus

The chemicals used in this work were purchased from Fluka and Merck Chemical Companies and used without purification. IR spectra were obtained as KBr pellets on a Perkin-Elmer 781 spectrophotometer and on an impact 400 Nicolet FT-IR spectrophotometer. ^{1}H NMR and ^{13}C NMR were recorded in $CDCl_3$ and DMSO solvents on a Bruker DRX-400 MHz spectrometer with tetramethylsilane as internal reference. A Bandelin ultrasonic HD 3200 with 6 mm diameter model KE 76 probe was used to generate ultrasonic irradiation and homogenize the reaction mixture. The piezoelectric crystals in this kind of probe normally work at approximately 700 kHz; by use of appropriate clamps. However, the output frequency of piezoelectric crystals was controlled and reduced to 20 kHz in the reaction mixture. XRD patterns were recorded by an X'PertPro (Philips) instrument with 1.54 °A wavelengths of X-ray beam and Cu anode material, at a scanning speed of 2° min^{-1} from 10° to 80° (2Ө). The SEM images of prepared catalysts were taken on a FE-SEM Hitachi S4160 instrument. The AFM image of GO nanosheets and functionalized graphene oxide were measured using scanning probe microscopy (SPM-9600, Shimadzu). Melting points obtained with a Yanagimoto micro melting point apparatus. The purity determination of the substrates and reaction monitoring were accomplished by TLC on silica-gel polygram SILG/UV 254 plates (from Merck Company).

4.1. Preparation of catalyst

Catalyst preparation involves several steps as followed:

4.1.1 Preparation of graphene oxide

Graphene oxide was synthesized by Hummers method.[37] Graphite powder (5.0 g) was stirred in the presence of sodium nitrate (2.5 g) and sulfuric acid (115 mL) placed in an ice bath. Then, potassium permanganate (15 g) was slowly added to mixture and stirred for 2 h. The mixture solution was transferred to a water bath (35 °C) and stirred for 30 min. Afterward of deionized water (230 mL) was added into the solution slowly and the solution temperature monitored was about 98 °C and stirred for 15 min. Then deionized water (700 mL) and H_2O_2 (50 mL, 30%) was added to the solution respectively. The obtained suspension was filtered and washed by diluted HCl (5%) and deionized water several times and dried at 60°C under vacuum. The graphite oxide was dispersed in distilled water to get a concentration of 0.5 mg mL^{-1} and exfoliated by ultrasound to obtain GO nanosheets.

4.1.2 Synthesis of 3-chloropropyltrimethoxysilane functionalized GO (GO@CTS)

Graphene oxide (1g) was dispersed in 250 mL anhydrous toluene by using an ultrasonic probe. Subsequently, 3.0 mL of CTS was diluted in 20 mL dry toluene that followed by drop wise addition to the graphene oxide dispersion. The reaction mixture was stirred and heated to reflux for 48 h under nitrogen atmosphere. After completion of the reaction, functionalized graphene oxide nanosheets were washed with toluene and ethanol to remove excess CTS and then dried under in an oven at 70 °C [38, 39].

4.1.3 Preparation of GO@N$_3$

In a 1000 mL round-bottom flask, 1.0 g of the GO@CTS was added into deionized water (150 mL), followed by sonication (35 W) for 5min. Then, 2g of NaN_3 and 0.2 g KI were added into the reaction vessel, heating at 60°C for 48 h. After this step, the resulted product was washed with water several times and dried at 50 °C in vacuum.

4.1.4 Huisgen 1,3-dipolar cycloaddition between azide functionalized GO (GO@N$_3$) and tripropargylamine

The azide functional GO, was attached to the alkyne groups by a copper catalyzed azide/alkyne “click” reaction (Scheme 1). The azide-functionalized GO (1g) was dispersed in 250 mL deionized water by using an ultrasonic probe. Subsequently, tripropargylamine(0.6 g) and copper catalyst based $CuSO_4$ and sodium ascorbate (0.05 and 0.1 equiv, respectively) were added into the reaction vessel. The reaction was performed for 48 h at room temperature. After this step, the resulted product was washed with water several times and dried under vacuum overnight.

4.1.5 Preparation of copper complex catalyst immobilized on GO(GO@PTA-Cu)

1,2,3-triazole-functionalized GO (1g) was dispersed in 250 mL dry acetonitrile by using ultrasonication. In the subsequent step, CuI (0.26 mmol, 0.05 g) was added to the stirring mixture. This mixture was refluxed for 24 h. After completion of the reaction, the immobilized catalyst was filtered and washed with CH_3CN and dried under vacuum overnight.

4.2 Typical procedure for the preparation of β-hydroxy-1,2,3-triazoles catalyzed by GO@PTA-Cu under ultrasound irradiation

A mixture of NaN_3 (72mg, 1.1mmol), epoxide (1mmol), alkyne (1mmol) and GO@PTA-Cu (10mg, 0.017mol%) in water (5mL) was sonicated at 45 kHz at room temperature for 7 min. After completion of the reaction, the solid product was dissolved in hot methanol and was filtered under reduced pressure using a vacuum pump over sintered glass. The solvent was eliminated under vacuum to give product 3a in 95% yield.

2-Phenyl-2-(4-phenyl-1H-1,2,3-triazol-1-yl)ethanol (3a). Pale yellow solid: mp. 125.0–127.0 °C, Lit.[40] (mp. 125.5–127.0 °C). IR (KBr): ν= 690, 758, 1047, 1080, 1241, 1438, 1463, 1493, 1593, 2928, 3065, 3089, 3140, 3345. ^{1}H NMR (400 MHz, $CDCl_3$) δ= 3.21 (t, J(H, H) = 6.8 Hz; 1H, OH), 4.22-4.27 (dd, 1H, ^3J(H–H) = 14.4 Hz, ^3J(H–H) = 3.6), 4.60-4.67 (dd, 1H, ^3J(H–H) = 12.4 Hz, ^3J(H–H) = 7.6), 5.69 (dd, ^3J(H–H) = 8 Hz, ^3J= 3.9 Hz, 1H), 7.33 (s, 1H), 7.38-7.42 (m, 6H), 7.70 (s, 1H), 7.79-7.80 (m, 3H).

2-(4-Phenyl-1H-1,2,3-triazol-1-yl)-2-p-tolylethanol (3b). Yellow solid: mp. 125.0–127.0 °C, Lit.[41] (mp. 124.0–126.0 °C). IR (KBr): ν= 697, 726, 757, 1047, 1075, 1008, 1185, 1221, 1380, 1457, 1497, 2927, 3028, 3092, 3417. ^{1}H NMR (400 MHz, $CDCl_3$) δ= 2.37 (t, J(H, H) = 2.8 Hz; 1H), 2.38 (s, 3H), 4.20-4.25 (dd, 1H, ^3J (H–H) = 9 Hz, ^3J (H–H) = 3.6), 4.61-4.65 (dd, 1H, ^3J (H–H) = 12.6 Hz, ^3J (H–H) = 8.4), 5.65-5.68 (dd, ^3J (H,H) = 8 Hz, ^3J= 3.2 Hz, 1H), 7.20-7.27 (m, 3H), 7.39 (m, 3H), 7.65-7.69(m, 3H).

1-(4-Phenyl-1H-1,2,3-triazol-1-yl)butan-2-ol (3c). White solid: mp. 110.0–112.0 °C, Lit.[35] (mp. 110.0–111.0 °C) IR (KBr): ν= 697, 763, 981, 1079, 1136, 1228, 1456, 1617, 2926, 2962, 3138, 3254, 3419. ^{1}H NMR(400 MHz, CDCl$_3$) δ= 1.05-1.09 (t, 3H), 1.53-1.66 (m, 2H), 2.65-2.66(d, ^3J(H–H) = 4.4, 1H), 4.1-4.27(m, 1H), 4.28-4.33 (dd, 1H, ^3J(H–H) = 13.8 Hz, ^2J(H–H) = 7.6), 4.50-4.55 (dd, 1H, ^3J(H–H) = 14 Hz), 7.34 (m, 1H), 7.40-7.43 (m, 2H), 7.79-7.80 (m, 2H), 7.87 (s, 1H).

1-Phenoxy-3-(4-phenyl-1H-1,2,3-triazol-1-yl)propan-2-ol (3d). Pale yellow solid: mp. 125.0–127.0 °C, Lit.[42] (mp. 125.5–126.0 °C). IR(KBr): ν= 692, 756, 981, 1043, 1245, 1494, 1595, 2866, 2927, 3087,3429. ^{1}H NMR (400 MHz, CDCl$_3$) δ= 3.76-3.94 (m, 1H), 4.04-4.22 (m, 2H), 4.54-4.56 (m, 2H), 4.73-4.75 (m, 1H), 6.91-6.93(m, 2H), 6.94-7.02 (m, 1H), 7.27-7.31 (m, 3H), 7.38-7.40 (m, 2H), 7.73-7.75 (m, 2H), 7.89 (s, 1H).

1-isopropoxy-3-(4-phenyl-1H-1,2,3-triazol-1-yl)propan-2-ol (3e). Yellow solid: mp. 62.0–64.0 °C, Lit.[35] (mp. 61.0–63.0) R (KBr): ν= 697, 765, 923, 975,1078, 1127, 1228, 1373, 1466, 2867, 2973, 3062, 3137, 3425.^{1}H NMR (400 MHz, CDCl$_3$) δ= 1.15–1.17 (d, 6H), 3.36-3.41 (dd, 1H, 3J(H–H) =10 Hz, ^3J(H–H) = 4), 3.51-3.53 (dd, 1H,^3J(H–H) = 8 Hz, ^3J(H–H) = 4.4), 3.57-3.64 (m, 1H), 4.21 (m, 1H), 4.40-4.64 (dd, 1H, 3J(H–H) = 14 Hz, 2J(H–H) = 4), 4.57-4.60 (dd, 1H, ^3J(H–H) =12 Hz, ^2J(H–H) = 2.8), 7.31-7.34 (m, 1H), 7.37-7.42 (m, 2H), 7.78-7.79 (m, 2H), 7.91 (s, 1H).

2-(4-Phenyl-1H-1,2,3-triazol-1-yl)cyclohexanol (3f). Yellow solid: mp. 168.0–172.0 °C, Lit. [40] (mp. 168.0–171.0 °C). IR (KBr): ν = 698, 768, 713, 1052, 1083, 1234, 1441, 2858, 2938, 3118, 3307. ^{1}H NMR (400 MHz, CDCl$_3$) δ= 0.9 (m, 2H), 1.26-1.51 (m, 4H), 1.91-2.01 (m, 2H), 4.09-4.11 (m, 1H), 4.16-4.19 (m, 1H), 7.3 (d, 1H), 7.72-7.74 (m, 2H), 7.79 (s, 1H).

2-Hydroxy-3-(4-phenyl-1H-1,2,3-triazol-1-yl)propyl acrylate (3g). Livid solid: mp. 102.0–104.0 °C, Lit.[35] (mp. 101.0–103.0 °C) IR (KBr): *ν*= 695, 756, 1044, 1245, 1494, 1596, 2925, 3087, 3426. ^{1}H NMR (400 MHz,$CDCl_3$) *δ*= 3.37-3.38 (dd, 1H), 3.95-4.07 (m, 2H), 4.55-4.65 (m, 2H), 4.73-4.79 (m, 1H), 6.91-6.92 (m, 2H), 6.98-7.02 (t, 1H), 7.31-7.35 (m, 2H), 7.40-7.43 (m, 2H), 7.77-7.79 (m, 1H), 7.91 (s, 1H).

1,3-Bis(4-phenyl-1H-1,2,3-triazol-1-yl)propan-2-ol (3h). Green solid: mp. 233.0–236.0 °C, Lit.[43] (mp. 233.0–236.0 °C).IR (KBr): *ν*= 687, 724, 763, 1074, 1126, 1278, 1464, 1729, 2861,2928, 2959. ^{1}H NMR (400 MHz, DMSO) *δ*= 4.40 (m, 2H), 4.56-4.61 (d, 1H), 5.81 (m, 1H), 7.30-7.32 (m, 1H), 7.42-7.44 (m, 2H), 7.84 (m, 2H), 8.55 (s, 1H). ^{13}C NMR (400) MHz, DMSO) *δ*= 54.84, 69.91, 124.12, 126.72, 127.11, 129.41, 129.68, 130.51, 132.42, 147.71.

1-(4-Phenyl-1H-1,2,3-triazol)hexan-2-ol (3i). Cream solid: mp. 92.0–94.0 °C, Lit.[41] (mp. 91.0–93.0 °C). IR (KBr): *ν*= 693, 764, 1087, 1138, 1228, 1463, 2862, 2925, 2959, 3142, 3248, 3407. ^{1}H NMR (400 MHz, $CDCl_3$) *δ*= 0.91-0.95 (t, 3H), 1.37-1.45 (m, 3H), 1.50-1.57 (m, 3H), 4.13-4.15 (m, 1H), 4.23-4.29 (m, 1H), 4.49-4.52 (m, 2H), 7.32-7.35 (m, 1H), 7.41-7.42 (m, 2H), 7.75-7.78 (m, 2H), 7.85 (s, 1H). ^{13}C NMR (400 MHz, $CDCl_3$) *δ*= 13.99, 22.59, 28.01, 34.17, 56.34, 70.44, 121.16, 125.53, 128.06, 128.78, 130.33, 147.27.

2-Phenyl-2-(4-propyl-1H-1,2,3-triazol-1-yl)ethanol (3j). Pale yellow solid: mp. 62.0–64.0 °C. IR (KBr): *ν*= 697, 761, 1070, 1280, 1455, 1726, 2853, 2925, 3061, 3367. ^{1}H NMR (400 MHz, $CDCl_3$) *δ*= 0.94 (m, 3H), 1.25-1.32 (m, 4H), 1.40-1.44 (m, 1H), 1.68–1.8 (t, 1H), 4.17-4.24 (m, 2H), 7.33-7.46 (m, 3H), 7.53-7.55 (m, 1H), 7.72 (m, 1H), 7.80 (s, 1H).

Acknowledgements

The authors are grateful to the University of Kashan for supporting this work by grant number 159148/77.

References

[1] P. Cintas, J.-L. Luche, Green Chem. 1 (1999) 115-125.

[2] V. Polshettiwar, R.S. Varma, Green Chem. 12 (2010) 743-754.

[3] C. Copéret, M. Chabanas, R. Petroff Saint-Arroman, J.M. Basset, Angew. Chem. Int. Ed. 42 (2003) 156-181.

[4] M. Meldal, C.W. Tornøe, Chem. Rev. 108 (2008) 2952-3015.

[5] T. Jin, M. Yan, Y. Yamamoto, ChemCatChem 4 (2012) 1217-1229.

[6] M. Nasr-Esfahani, I. Mohammadpoor-Baltork, A.R. Khosropour, M. Moghadam, V. Mirkhani, S. Tangestaninejad, H. Amiri Rudbari, J. Org. Chem. 79 (2014) 1437-1443.

[7] X. Xiong, L. Cai, Y. Jiang, Q. Han, Eng 2 (2014) 765-771.

[8] R.P. Jumde, C. Evangelisti, A. Mandoli, N. Scotti, R. Psaro, J. Catal. 324 (2015) 25-31.

[9] M. Chetia, A.A. Ali, D. Bhuyan, L. Saikia, D. Sarma, New J. Chem. 39 (2015) 5902-5907.

[10] A.S. Kumar, M.A. Reddy, M. Knorn, O. Reiser, B. Sreedhar, Eur. J. Org. Chem. 2013 (2013) 4674-4680.

[11] A. Shaygan Nia, S. Rana, D. Döhler, F. Jirsa, A. Meister, L. Guadagno, E. Koslowski, M. Bron, W.H. Binder, Chem. Eur. J. 21 (2015) 10763-10770.

[12] H. Sharghi, M. Hosseini-Sarvari, F. Moeini, R. Khalifeh, A.S. Beni, Helv. Chim. Acta 93 (2010) 435-449.

[13] Q. Yue, Y. Zhang, C. Wang, X. Wang, Z. Sun, X.-F. Hou, D. Zhao, Y. Deng, J. Mater. Chem. A 3 (2015) 4586-4594.

[14] Z. Wang, X. Yang, J. Yang, Y. Jiang, N. He, Anal. Chim. Acta 862 (2015) 53-63.

[15] W. Zhang, J. Chen, R. Liu, S. Wang, L. Chen, K. Li, ACS Sustainable Chem. Eng. 2 (2014) 683-691.

[16] Y. Tonbul, M. Zahmakiran, S. Özkar, Appl. Catal., B 148 (2014) 466-472.

[17] N. Salam, B. Banerjee, A.S. Roy, P. Mondal, S. Roy, A. Bhaumik, S.M. Islam, Appl. Catal., A 477 (2014) 184-194.

[18] J. Mondal, A. Biswas, S. Chiba, Y. Zhao, Sci. Rep. 5 (2015).

[19] W. Chen, J. Ji, X. Duan, G. Qian, P. Li, X. Zhou, D. Chen, W. Yuan, Chem. Commun. 50 (2014) 2142-2144.

[20] N.M. Julkapli, S. Bagheri, Int. J. Hydrogen Energy 40 (2015) 948-979.

[21] R.H. Fath, S.J. Hoseini, J. Organomet. Chem. 828 (2017) 16-23.

[22] O.C. Compton, S.T. Nguyen, small 6 (2010) 711-723.

[23] D.R. Dreyer, S. Park, C.W. Bielawski, R.S. Ruoff, Chem. Soc. Rev. 39 (2010) 228-240.

[24] K. Haubner, J. Murawski, P. Olk, L.M. Eng, C. Ziegler, B. Adolphi, E. Jaehne, Chemphyschem 11 (2010) 2131-2139.

[25] K.P. Loh, Q. Bao, P.K. Ang, J. Yang, J. Mater. Chem. 20 (2010) 2277-2289.

[26] S. Park, R.S. Ruoff, Nat. Nanotechnol. 4 (2009) 217-224.

[27] S. Stankovich, R.D. Piner, S.T. Nguyen, R.S. Ruoff, Carbon 44 (2006) 3342-3347.

[28] L. Wang, D. Wang, S. Zhang, H. Tian, Catal. Sci. Technol. 3 (2013) 1194-1197.

[29] Y. Yang, J. Wang, J. Zhang, J. Liu, X. Yang, H. Zhao, Langmuir 25 (2009) 11808-11814.

[30] W.G. Lewis, F.G. Magallon, V.V. Fokin, M. Finn, J. Am. Chem. Soc. 126 (2004) 9152-9153.

[31] T.R. Chan, R. Hilgraf, K.B. Sharpless, V.V. Fokin, Org. Lett. 6 (2004) 2853-2855.

[32] N. Candelon, D. Lastécouères, A.K. Diallo, J.R. Aranzaes, D. Astruc, J.-M. Vincent, Chem. Commun. (2008) 741-743.

[33] S. z ubuk u , E. Ozkal, C. Jimeno, M.A. Pericas, Org. Lett. 11 (2009) 4680-4683.

[34] J.M. Gónzalez-Dominguez, M. Gonzalez, A. Anson-Casaos, A. Diez-Pascual, M. Gomez, M. Martinez, J. Phys. Chem. C 115 (2011) 7238-7248.

[35] H. Naeimi, V. Nejadshafiee, New J. Chem. 38 (2014) 5429-5435.

[36] J.E. Hein, J.C. Tripp, L.B. Krasnova, K.e.B. Sharpless, V.V. Fokin, Angew. Chem. 121 (2009) 8162-8165.

[37] S. William, J. Hummers, R.E. Offeman, J. Am. Chem. Soc. 80 (1958) 1339.

[38] M.A. Nasseri, A. Allahresani, H. Raissi, RSC Adv. 4 (2014) 26087-26093.

[39] H.P. Mungse, S. Verma, N. Kumar, B. Sain, O.P. Khatri, J. Mater. Chem. 22 (2012) 5427-5433.

[40] F. Alonso, Y. Moglie, G. Radivoy, M. Yus, J. Org. Chem. 76 (2011) 8394-8405.

[41] J. Yadav, B.S. Reddy, G.M. Reddy, D.N. Chary, Tetrahedron Lett. 48 (2007) 8773-8776.

[42] H. Sharghi, M.H. Beyzavi, A. Safavi, M.M. Doroodmand, R. Khalifeh, Adv. Synth. Catal. 351 (2009) 2391-2410.

[43] T. Boningari, A. Olmos, B.M. Reddy, J. Sommer, P. Pale, Eur. J. Org. Chem. 2010 (2010) 6338-6347.

Graphical Abstract

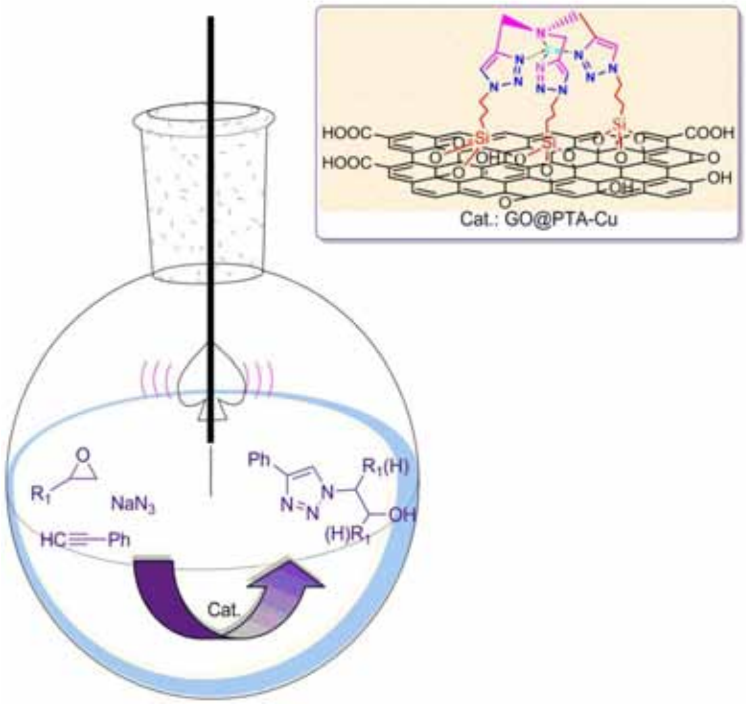

In the present study, a copper complex immobilized on graphene oxide was synthesized as a novel, green, highly efficient and heterogeneous reusable catalyst. Then, the synthesis of *β*-hydroxy-1,2,3-triazole derivatives were performed by the employment of GO@polytriazole-Cu as catalyst under ultrasound irradiation to afford the desired products in high yields and short reaction time.